

Uniform Magnetic Core/Shell Microspheres Functionalized with Ni²⁺–Iminodiacetic Acid for One Step Purification and Immobilization of His-Tagged Enzymes

Yuting Zhang,[†] Yongkun Yang,[‡] Wanfu Ma,[†] Jia Guo,[†] Yao Lin,^{*,‡} and Changchun Wang^{*,†}

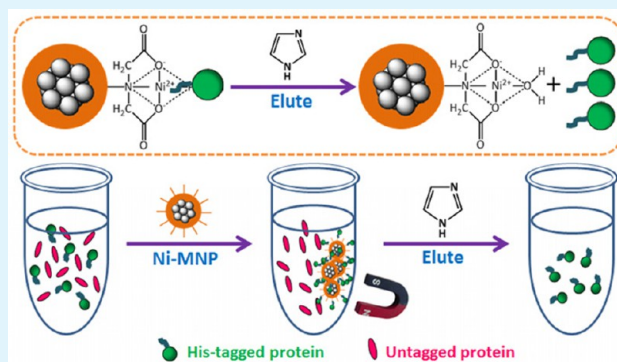
[†]State Key Laboratory of Molecular Engineering of Polymers, Department of Macromolecular Science, and Laboratory of Advanced Materials, Fudan University, Shanghai 200433, People's Republic of China

[‡]Polymer Program, Institute of Materials Science and Department of Chemistry, University of Connecticut, Storrs, Connecticut 06269, United States

S Supporting Information

ABSTRACT: A facile approach has been developed to synthesize Fe₃O₄/PMG (poly (*N,N'*-methylenebisacrylamide-*co*-glycidyl methacrylate)) core/shell microspheres using distillation–precipitation polymerization. Treating PMG shell with iminodiacetic acid (IDA) and Ni²⁺ yields composite microspheres of Fe₃O₄/PMG/IDA–Ni²⁺. The Ni²⁺ ions loaded on the surface of microspheres provide abundant docking sites for immobilization of histidine-tagged proteins. The high saturation magnetization of Fe₃O₄/PMG (23 emu/g), determined by vibrating sample magnetometer (VSM), allows an easy separation of the microspheres from solution under an external magnetic field. The composite microspheres were used to purify two His-tagged cellulolytic enzymes (Cel48F and Cel9G) directly from crude cell lysates with high binding affinity, capacity, and specificity. The microspheres can be recycled for many times without significant loss of binding capacity to enzymes. The immobilized enzymes on the surface of microspheres well retain their biological activities in degradation of cellulose. These materials show great potential in the biomedical and biotechnological applications that require low-cost purification of recombinant proteins and instant enzyme immobilization at an industrial scale.

KEYWORDS: Fe₃O₄/PMG core/shell microspheres, purification, His-tagged protein, enzyme immobilization, cellulase, cellulosome



1. INTRODUCTION

Magnetic composite microspheres have been extensively investigated owing to their excellent magnetic responsiveness and their applications in protein purification,^{1,2} cell separation,^{3,4} medical diagnosis,^{5–7} and targeted drug delivery.^{8–10} Among different types of magnetic composite microspheres, magnetic polymeric microspheres (MPMs) with high magnetic susceptibility and tailored functional polymer shell have attracted special attention. Emulsion polymerizations, such as conventional emulsion polymerization,¹¹ soap-free emulsion polymerization,¹² miniemulsion polymerization,¹³ and microemulsion polymerization¹⁴ are routinely used to prepare MPMs with specific composite structures. Traditionally, the polymer shells in MPMs are made by the copolymerization of styrene or acrylic monomers with other functional monomers.¹⁵ However, the hydrophobic nature of these polymer shells limit the subsequent biological applications.¹⁶ Recently, distillation–precipitation polymerization (DPP) has been developed to synthesize MPMs coated with hydrophilic polymers^{17–20} containing carboxylic acid,²¹ sulfonic acid,²² or pyridyl group²³ with precise control over their densities. The

hydrophilic MPMs synthesized by DPP show great promise in the biological applications such as the separation and purification of recombinant proteins.

With the fast development of proteomics and protein-based biotechnologies, efficient separation and purification of recombinant proteins in a cost-effective way are urgently needed.^{24–26} Immobilized metal-ion affinity chromatography (IMAC),²⁷ which employs iminodiacetic acid (IDA) or nitrilotriacetic acid (NTA) groups to immobilize nickel ions (Ni²⁺), is widely used in the purification of recombinant proteins containing six consecutive histidine residues (His-tag) at the N- or C-terminus. For some specific applications, however, it is highly desired to separate His-tagged proteins directly from crude cell lysates, using magnetic nanoparticles or microspheres.^{28–30} In the past few years, much effort has been made to develop magnetic nanoparticle-based³¹ platforms for the purification of His-tagged proteins.^{32–40} However, the small

Received: January 5, 2013

Accepted: March 7, 2013

Published: March 7, 2013

diameters (~ 10 nm) of magnetic particles used in many studies made it difficult to quickly separate the particles from the solution. To address the problem, Zheng and co-workers⁴¹ applied relatively large Fe_3O_4 core (~ 200 nm) in the synthesis of core/shell microspheres with Ni-NTA moiety on the surface. However, an additional layer of SiO_2 was needed in the synthesis to coat the polymers on the particle surface.

Herein, we report a facile method to prepare magnetic microspheres of Fe_3O_4 /PMG(poly (*N,N'*-methylenebisacrylamide-co-glycidyl methacrylate))/IDA- Ni^{2+} with a core of magnetic colloidal nanocrystal clusters (MCNCs) and a shell of hydrophilic polymer. We then demonstrate the use of the microspheres in one-step purification and immobilization of His-tagged cellulolytic enzymes for biotechnological applications. Compared with the magnetic nanoparticles, the as-prepared composite microspheres have much higher magnetic susceptibility and an excellent binding capacity of His-tagged proteins. For the two cellulolytic enzymes we examined, the composite microspheres show excellent binding selectivity against other *E. coli* proteins in the crude cell lysate. The microspheres can be recycled for many times without significant loss of binding capacity to enzymes. We also found that the immobilized enzymes on the surface of microspheres could well retain their biological activities in the degradation of cellulose.

2. EXPERIMENTAL SECTION

2.1. Materials. Iron(III) chloride hexahydrate ($\text{FeCl}_3 \cdot 6\text{H}_2\text{O}$), ammonium acetate (NH_4Ac), ethylene glycol (EG), anhydrous ethanol, trisodium citrate dihydrate, aqueous ammonia solution (25%), sodium chloride (NaCl), and tris (hydroxymethyl) amino-methane (Tris) were purchased from Shanghai Chemical Reagents Company. Trizma maleate, calcium chloride, potassium ferricyanide, potassium cyanide, ferric ammonium sulfate, sodium dodecyl sulfate, sulfuric acid, and glucose were purchased from Sigma-Aldrich Co. LLC. Sodium carbonate and ferric chloride were purchased from Fisher Scientific Inc. Imidazole was purchased from Aladdin. Glycidyl methacrylate (GMA) was obtained from Aldrich and vacuum distilled. *N,N'*-Methylenebisacrylamide (MBA) was bought from Fluka and recrystallized from acetone. 2,2-Azobisisobutyronitrile (AIBN) was purchased from Sinopharm Chemical Reagents Company and recrystallized from ethanol. Iminodiacetic acid (IDA), sodium hydroxide (NaOH), and nickel(II) chloride hexahydrate ($\text{NiCl}_2 \cdot 6\text{H}_2\text{O}$) were purchased from Sinopharm Chemical Reagents Company. γ -Methacryloxypropyltrimethoxy-silane (MPS) was obtained from Jiangsu Chen Guang Silane Coupling Reagent Co., Ltd. Acetonitrile (AN) was purchased from Shanghai Ling-feng Chemical Reagent Company. Deionized water was used in all the experiments. Avicel PH101 was purchased from Fluka Analytical.

2.2. Preparation of MCNCs Stabilized by Sodium Citrate. Magnetic colloidal nanocrystal clusters (MCNCs) were prepared by a modified solvothermal reaction. Specifically, 1.350 g of $\text{FeCl}_3 \cdot 6\text{H}_2\text{O}$, 3.854 g of NH_4Ac , and 0.400 g of trisodium citrate dihydrate were dissolved in 70 mL of ethylene glycol. The mixture was stirred vigorously for 1 h at 160 °C to form a black, homogeneous solution and then transferred into a Teflon-lined stainless-steel autoclave. The autoclave was heated at 200 °C and maintained for 16 h, before it was cooled to room temperature. The resulting MCNCs were washed several times with ethanol and redispersed in ethanol for the subsequent use. The magnetic nanoparticles synthesized were around 200 nm in diameter.

2.3. Modification of the Fe_3O_4 with MPS. The Fe_3O_4 microspheres were modified with γ -methacryloxypropyltrimethoxy-silane (MPS) to form abundant double bonds on the surface. The modification is generally as follows: 40 mL of ethanol, 10 mL of deionized water, 1.5 mL of $\text{NH}_3 \cdot \text{H}_2\text{O}$, and 0.6 g of MPS were mixed with 300 mg of Fe_3O_4 . Then, the mixture was stirred vigorously for 24

h at 70 °C. The obtained product was separated by a magnet and washed by ethanol for several times to remove excess MPS. The resultant Fe_3O_4 /MPS was dried in a vacuum oven at 40 °C until it was a constant weight.

2.4. Synthesis of Fe_3O_4 /PMG Core/Shell Microspheres by DPP Method. The core/shell Fe_3O_4 /PMG microspheres were prepared via one-step distillation-precipitation polymerization (DPP) of GMA in acetonitrile, by adding MBA as the cross-linker and AIBN as the initiator. Typically, 50 mg of Fe_3O_4 /MPS seed microspheres were dispersed in 40 mL of acetonitrile in a dried 100 mL single-necked flask under ultrasonic condition for 3 min. Then, a mixture of 150 mg of GMA, 150 mg of MBA, and 6 mg of AIBN was added to the flask to initiate the polymerization. The flask submerged in a heating oil bath was attached with a fractionating column, Liebig condenser, and a receiver. The reaction mixture was heated from room temperature to the boiling state within 30 min, and the reaction was complete after 20 mL of acetonitrile was distilled from the reaction mixture in about 1 h. The obtained Fe_3O_4 /PMG microspheres were collected by magnetic separation and washed repeatedly with ethanol and water.

2.5. Preparation of Fe_3O_4 /PMG/IDA Microspheres. Iminodiacetic acid (IDA) was used to open the epoxy ring of GMA on the surface of the composite microspheres. Specifically, 0.33 g of IDA and 0.2 g of NaOH were dissolved in 20 mL of deionized water under stirring. The pH of the solution was adjusted to 11 with NaOH solution (2M). Subsequently, 50 mg of Fe_3O_4 /PMG microspheres was added to the solution, and the mixture was stirred vigorously for 12 h at 80 °C. The obtained microspheres were separated by a magnet and washed by ethanol and water for several times.

2.6. Preparation of Fe_3O_4 /PMG/IDA- Ni^{2+} Microspheres. Fe_3O_4 /PMG/IDA (50 mg) was added to a 10 mL NiCl_2 solution (0.1 M) and stirred for 2 h at room temperature. The product was separated from the solution and washed several times with water. The resultant Fe_3O_4 /PMG/IDA- Ni^{2+} microspheres were dried in a vacuum oven at 40 °C.

2.7. His-Tagged Protein Binding and Separation. The Fe_3O_4 /PMG/IDA- Ni^{2+} magnetic particle suspension (100 μL , 2 mg/mL) was sedimented on a magnetic plate and washed with 100 μL of buffer solution I (50 mM Tris, pH 8.0, 300 mM NaCl , 5 mM imidazole) for three times. Protein solution (100 μL , 0.433 mg/mL) was then mixed with the magnetic microspheres and incubated at room temperature for 30 min. After incubation, the supernatant was removed using a pipet, and the protein-bonded composite microspheres were washed twice with 100 μL of buffer solution I. The protein was eluted from the composite microspheres with 50 μL of buffer solution II (50 mM Tris, pH 8.0, 300 mM NaCl , 300 mM imidazole). The protein solutions from each step were analyzed by UV-vis and sodium dodecyl sulfate (SDS)-polyacrylamide gel electrophoresis (PAGE).

2.8. Expression and Purification of His-Tagged Proteins from Cell Lysate. The genes encoding the cellulases Cel48F⁴² and Cel9G⁴³ from *Clostridium cellulolyticum* were codon optimized for *E. coli* and synthesized by GenScript Corporation. The genes were then ligated into pET28b(+) vector between the *NheI* and *XhoI* restriction sites following the N-terminal His-tag and thrombin cleavage site. The protein-encoding plasmids were transformed into BL21(DE3) cells (Invitrogen) using standard protocol. The transformed BL21(DE3) cells were incubated in LB media with kanamycin by shaking at 37 °C until $\text{OD}_{600} = 1.0-1.2$, at which time the temperature was lowered to 18 °C (Cel48F) or 15 °C (Cel9G), and isopropyl thio- β -D-galactoside was added to a final concentration of 40 μM . After 16 h, the cells were harvested by centrifugation at 4000g and 4 °C and stored at -80 °C.

The frozen cell pellet was resuspended in 1 \times BugBuster protein extraction reagent (Novagen, USA) supplemented with Benzonase Nuclease and rLysozyme and incubated at room temperature for 15 min. The clear cell lysate (L) was obtained by centrifugation at 16 000g for 20 min at 4 °C. Before mixing with the cell lysate, 500 μL of Fe_3O_4 /PMG/IDA- Ni^{2+} (10 mg/mL) was washed by the lysis buffer (50 mM Tris, pH 8.0, 300 mM NaCl , 5 mM imidazole) twice. Then, 1 mL of cell lysate was incubated with the washed magnetic microspheres Fe_3O_4 /PMG/IDA- Ni^{2+} (Ni-MNPs) at 4 °C for 30

Scheme 1. Fabrication Procedures of $\text{Fe}_3\text{O}_4/\text{PMG}/\text{IDA}-\text{Ni}^{2+}$ Microspheres and Their Application in Selective Enrichment of His-Tagged Proteins

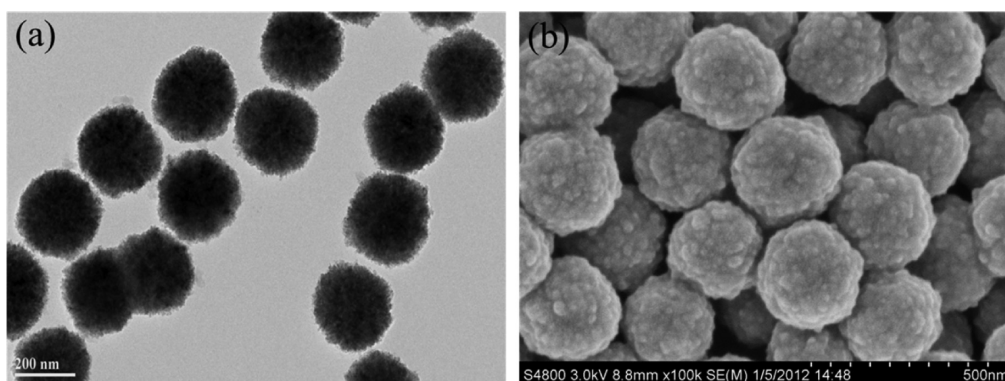
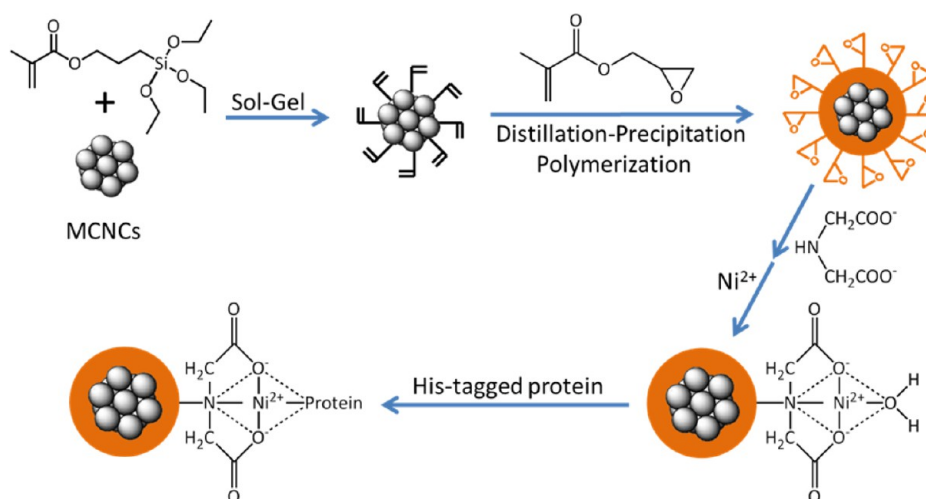


Figure 1. (a) TEM and (b) SEM images of magnetic colloid nanocrystal clusters (MCNCs). The scale bar is 200 nm in (a) and 500 nm in (b).

min. After the Ni-MNPs were completely sedimented by magnetic plate, the supernatant was removed by pipet. The Ni-MNPs were resuspended in 1 mL of lysis buffer (50 mM Tris, pH 8.0, 300 mM NaCl, 5 mM imidazole) and separated from the buffer by magnetic sedimentation again after 1 min. The resuspension and sedimentation steps were repeated using 250 μL buffers containing 5, 20, 30, 40, 80, 120, 160, 200, 250, 300, and 500 mM imidazole sequentially. The protein solutions in each step were analyzed by SDS-PAGE.

2.9. Enzyme Activity. Kinetic studies of cellulose hydrolysis were performed by incubating the protein samples with 20 mg/mL microcrystalline cellulose (Avicel PH101, Fluka) in 5 mM Tris maleate, pH 6.0, 1 mM CaCl_2 , 0.01% (w/v) NaN_3 at 37 $^\circ\text{C}$. The final protein concentration was 0.02 μM for all experiments. Aliquots (0.9 mL) were extracted at 0, 1, 6, and 24 h, centrifuged, and examined for soluble reducing sugars using ferricyanide assay.⁴⁴

2.10. Characterization. High-resolution transmission electron microscopy (HR-TEM) images were taken on a JEM-2100F transmission electron microscope at an accelerating voltage of 200 kV. Samples dispersed at an appropriate concentration were cast onto a carbon-coated copper grid. Field-emission scanning electron microscopy (FE-SEM) was performed on a Hitachi S-4800 scanning electron microscope at an accelerating voltage of 20 kV. Sample dispersed at an appropriate concentration was cast onto a glass sheet at room temperature and sputter-coated with gold. X-ray diffraction (XRD) was performed on a Panalytical X'Pert Pro diffraction meter. Magnetic characterization was carried out on a vibrating sample magnetometer (VSM) on a Model 6000 physical property measurement system (Quantum, USA) at 300 K. Hydrodynamic diameter (D_h) measurements were conducted by dynamic light scattering (DLS) with a ZEN3600 (Malvern, UK) Nano ZS instrument using

He-Ne laser at a wavelength of 632.8 nm. Fourier transform infrared spectra (FT-IR) were determined on a NEXUS-470 FT-IR spectrometer. Spectra were scanned over the range of 400–4000 cm^{-1} . All of the dried samples were mixed with KBr and then compressed to form pellets. Thermogravimetric analysis (TGA) measurements were performed on a Pyris 1 TGA instrument. All measurements were taken under a constant flow of nitrogen of 40 mL/min. The temperature was first increased from room temperature to 100 $^\circ\text{C}$, held until constant weight, and then increased from 100 to 800 $^\circ\text{C}$ at a rate of 20 $^\circ\text{C}/\text{min}$. Atomic absorption spectrometer (AAS) measurements were taken on a Z-5000 AAS instrument. SDS-PAGE was performed using 4–15% precast polyacrylamide gels and Mini-PROTEAN Tetra cell (Bio-Rad, USA). Protein concentration was obtained by measuring absorbance at 280 nm using a Thermo Scientific Nanodrop 2000 spectrophotometer.

3. RESULTS AND DISCUSSION

The preparation of composite microspheres containing a superparamagnetic MCNCs core and a polymer shell with abundant Ni^{2+} was schematically illustrated in Scheme 1. First, MCNCs (about 200 nm) were synthesized by a modified solvothermal reaction; second, the MCNCs were modified with MPS to form active double bonds on the surface, which are essential for the polymer attachment in the next step; third, a layer of PMG was coated on the $\text{Fe}_3\text{O}_4/\text{MPS}$ core by distillation–precipitation polymerization (DPP) of GMA (monomer) and MBA (cross-linker) to form $\text{Fe}_3\text{O}_4/\text{PMG}$ core–shell microspheres; finally, IDA was added to react with

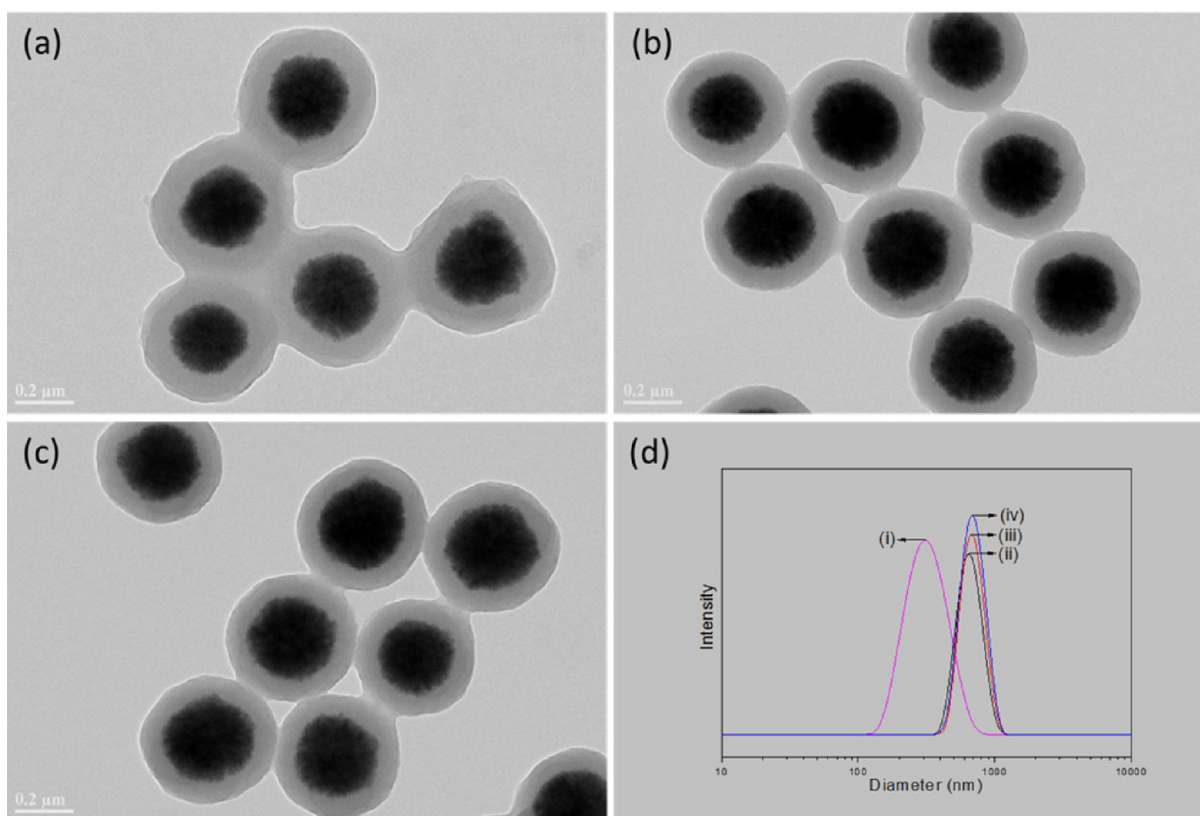


Figure 2. TEM images of (a) $\text{Fe}_3\text{O}_4/\text{PMG-1}$, (b) $\text{Fe}_3\text{O}_4/\text{PMG-2}$, and (c) $\text{Fe}_3\text{O}_4/\text{PMG-3}$ (all scale bars are $0.2 \mu\text{m}$); (d) DLS plots of (i) $\text{Fe}_3\text{O}_4/\text{MPS}$, (ii) $\text{Fe}_3\text{O}_4/\text{PMG-1}$, (iii) $\text{Fe}_3\text{O}_4/\text{PMG-2}$, and (iv) $\text{Fe}_3\text{O}_4/\text{PMG-3}$.

Table 1. Recipes and Particle Sizes of $\text{Fe}_3\text{O}_4/\text{PMG}$ with Different Feeding Amounts of GMA

sample code	GMA/mg	MBA/mg	AIBN/mg	D_h/nm	PDI
$\text{Fe}_3\text{O}_4/\text{PMG-1}$	50	150	4.0	603	0.194
$\text{Fe}_3\text{O}_4/\text{PMG-2}$	100	150	5.0	752	0.051
$\text{Fe}_3\text{O}_4/\text{PMG-3}$	150	150	6.0	792	0.055

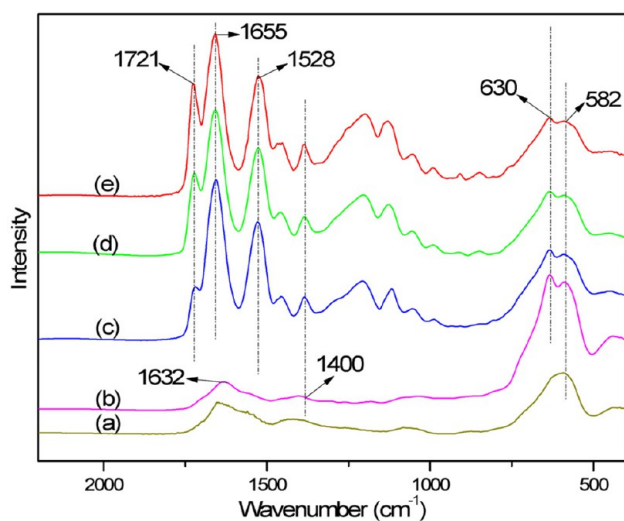


Figure 3. FT-IR spectra of (a) Fe_3O_4 , (b) $\text{Fe}_3\text{O}_4/\text{MPS}$, (c) $\text{Fe}_3\text{O}_4/\text{PMG-1}$, (d) $\text{Fe}_3\text{O}_4/\text{PMG-2}$, and (e) $\text{Fe}_3\text{O}_4/\text{PMG-3}$.

the epoxy ring of GMA and immobilize Ni^{2+} on the surface of the microspheres.

3.1. Preparation of MCNCs Stabilized by Sodium Citrate.

Water-dispersible MCNCs were produced by a modified solvothermal reaction at 200°C with hexahydrated iron(III) chloride ($\text{FeCl}_3 \cdot 6\text{H}_2\text{O}$) as the precursor, NH_4Ac as the alkali source, trisodium citrate (Na_3Cit) as the electrostatic stabilizer, and EG as both the reducing agent and the solvent. The TEM image shows that the MCNCs have a mean diameter of about 200 nm (Figure 1a). The MCNCs are uniform in both shape and size. The SEM image (Figure 1b) indicates that the magnetic clusters consist of many small nanocrystals, which is consistent with previous literature.^{45,46} X-ray diffraction (XRD) experiments (Supporting Information, Figure S1) were carried out to determine the composition of MCNCs and the average grain size. All the diffraction peaks in the XRD patterns were indexed and assigned to the typical cubic structure of Fe_3O_4 (JCPDS 75-1609). No diffraction peaks from hematite or other impurities were detected, indicating the formation of pure magnetite products.

3.2. Synthesis of $\text{Fe}_3\text{O}_4/\text{PMG}$ Core/Shell Microspheres by DPP method.

PMG shell coated on $\text{Fe}_3\text{O}_4/\text{MPS}$ was prepared by the distillation–precipitation polymerization method to directly encapsulate MCNCs. In our previous report, we demonstrated that a variety of monomers including methylacrylic acid (MAA), acrylic acid (AA), *N*-isopropylacrylamide (NIPAM), and acrylic amide (AM) can be used to make hydrophilic polymers on MCNCs by the DPP method.⁴⁷ Here, we come up with a different approach which uses hydrophobic instead of hydrophilic monomers to prepare magnetic polymeric microspheres with abundant epoxy groups on the surface. The mechanism is as follows: as PMG species are not soluble in acetonitrile, the generated PMG oligomers will

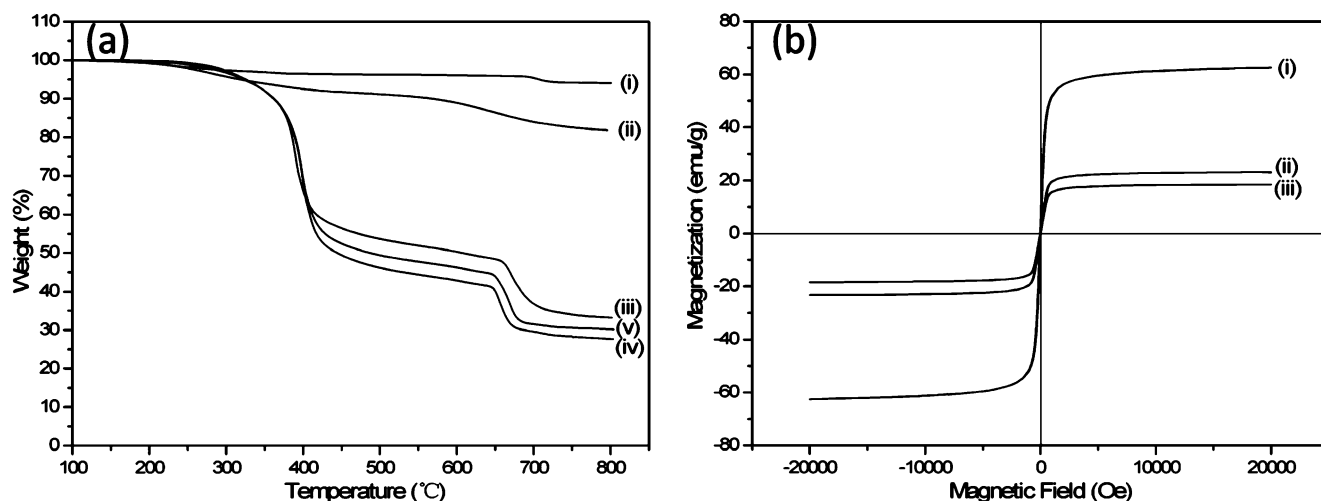
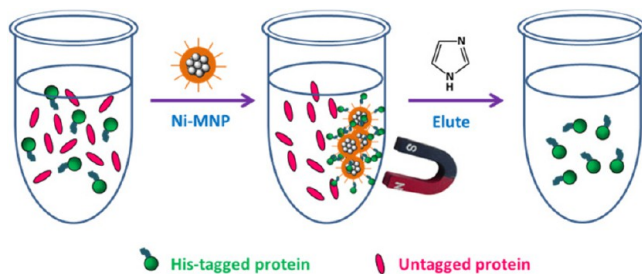


Figure 4. (a) TGA curves of (i) Fe_3O_4 , (ii) $\text{Fe}_3\text{O}_4/\text{MPS}$, (iii) $\text{Fe}_3\text{O}_4/\text{PMG-3}$, (iv) $\text{Fe}_3\text{O}_4/\text{PMG-IDA-3}$, and (v) $\text{Fe}_3\text{O}_4/\text{PMG-IDA-Ni}^{2+}$ -3. (b) Magnetic hysteresis curves of (i) $\text{Fe}_3\text{O}_4/\text{MPS}$, (ii) $\text{Fe}_3\text{O}_4/\text{PMG-3}$, and (iii) $\text{Fe}_3\text{O}_4/\text{PMG-IDA-Ni}^{2+}$ -3.

Table 2. Loading Amounts of Ni^{2+} in Different Samples of $\text{Fe}_3\text{O}_4/\text{PMG}/\text{IDA-Ni}^{2+}$

sample code	Ni^{2+} loading amount (mg/g)
$\text{Fe}_3\text{O}_4/\text{PMG}/\text{Ni}^{2+}$	0
$\text{Fe}_3\text{O}_4/\text{PMG-1}/\text{IDA-Ni}^{2+}$ (Ni-MNPs-1)	32
$\text{Fe}_3\text{O}_4/\text{PMG-2}/\text{IDA-Ni}^{2+}$ (Ni-MNPs-2)	55
$\text{Fe}_3\text{O}_4/\text{PMG-3}/\text{IDA-Ni}^{2+}$ (Ni-MNPs-3)	57

Scheme 2. Separation and Purification Procedure of His-Tagged Proteins from Crude Cell Lysate



continuously precipitate from the solution and attach to the surface of the MCNCs to form a robust shell with the simultaneous distillation of the solvent. A careful control over the distillation rate will result in the encapsulation of MCNCs with a uniform polymer layer, while keeping the system from the aggregations.

The density of the functional groups on the surface can be tuned in the synthesis for the specific requirements in the downstream biological applications. We attempted to control the surface density of the epoxy groups on the microspheres by changing the feeding amount of GMA. We kept the weight of MBA constant (150 mg) and increased the dosage of GMA from 0 to 200 mg. Without GMA, the shell polymerized from MBA has poor structural integrity (data not shown). When the dosage of GMA was increased (from 50 mg to 100 mg and to 150 mg, as in Figure 2a–c), the thickness of the polymeric shell remained unchanged while the shape became more uniform. However, when the weight of GMA increased to 200 mg, the thickness of the shell decreased and became less uniform (data not shown). Accordingly, the hydrodynamic diameter and size distribution of microspheres were determined in situ by

dynamic light scattering (DLS). As shown in Figure 2d, the hydrodynamic diameter (D_h) of MCNCs is around 290 nm, which is very close to the size measured by TEM. The D_h of $\text{Fe}_3\text{O}_4/\text{PMG}$ increased when the dosage of GMA changed from 50 to 100 and to 150 mg (Figure 2d and Table 1). The polydispersity indexes (PDI) of $\text{Fe}_3\text{O}_4/\text{MPS}$, $\text{Fe}_3\text{O}_4/\text{PMG-1}$, $\text{Fe}_3\text{O}_4/\text{PMG-2}$, and $\text{Fe}_3\text{O}_4/\text{PMG-3}$ are all around 0.1, indicating that all the particles are uniform.

The functional groups in the polymer shell were analyzed by FT-IR. As shown in Figure 3, the peaks at 1721 and 1528 cm^{-1} are attributed to the stretching vibration of $\text{C}=\text{O}$ of the ester group in GMA and bending vibration of N-H in MBA, respectively. The intensity of the $\text{C}=\text{O}$ peak is enhanced with increasing amount of GMA, with $\text{Fe}_3\text{O}_4/\text{PMG-3}$ being the strongest. We chose $\text{Fe}_3\text{O}_4/\text{PMG-3}$ for the further characterization of its composition and magnetic property, with the expectation that the sample can incorporate the largest amount of Ni^{2+} on the surface.

The composition of the composite microspheres was studied by thermogravimetric analysis (TGA). The TGA curves in each step were shown in Figure 4a. The weight loss of Fe_3O_4 (6 wt %) was attributed to the stabilizer sodium citrate, and the weight loss of $\text{Fe}_3\text{O}_4/\text{MPS}$ (18 wt %) was attributed to the sodium citrate and MPS. The different weight losses confirmed the formation of MPS layer on the surface of Fe_3O_4 . Besides the organic components in $\text{Fe}_3\text{O}_4/\text{MPS}$, the PMG layer of $\text{Fe}_3\text{O}_4/\text{PMG}$ can also lose weight upon heating. The weight loss of $\text{Fe}_3\text{O}_4/\text{PMG-3}$ is around 67 wt %, indicating a magnetite content of about 33 wt % in $\text{Fe}_3\text{O}_4/\text{PMG-3}$. It is worth mentioning that the TGA profile for $\text{Fe}_3\text{O}_4/\text{PMG-3}$ had a pronounced step around $650\text{ }^\circ\text{C}$, which did not show up in $\text{Fe}_3\text{O}_4/\text{MPS}$. We believe this peak may be attributed to the weight loss of partial PMG chains that are directly attached to the surface of MCNCs, and the remarkably increased temperature reflects the strong interactions between the polymer chains and the surface of MCNCs.⁴⁷ The magnetic properties of $\text{Fe}_3\text{O}_4/\text{MPS}$ and $\text{Fe}_3\text{O}_4/\text{PMG-3}$ were determined by vibrating sample magnetometer (VSM) (Figure 4b). The saturation magnetization (M_s) value of $\text{Fe}_3\text{O}_4/\text{MPS}$ was 63 emu/g. After encapsulation with a layer of PMG, the value decreased to 23 emu/g. This result indicates that the effective magnetic content in the composite microspheres is 37 wt %,

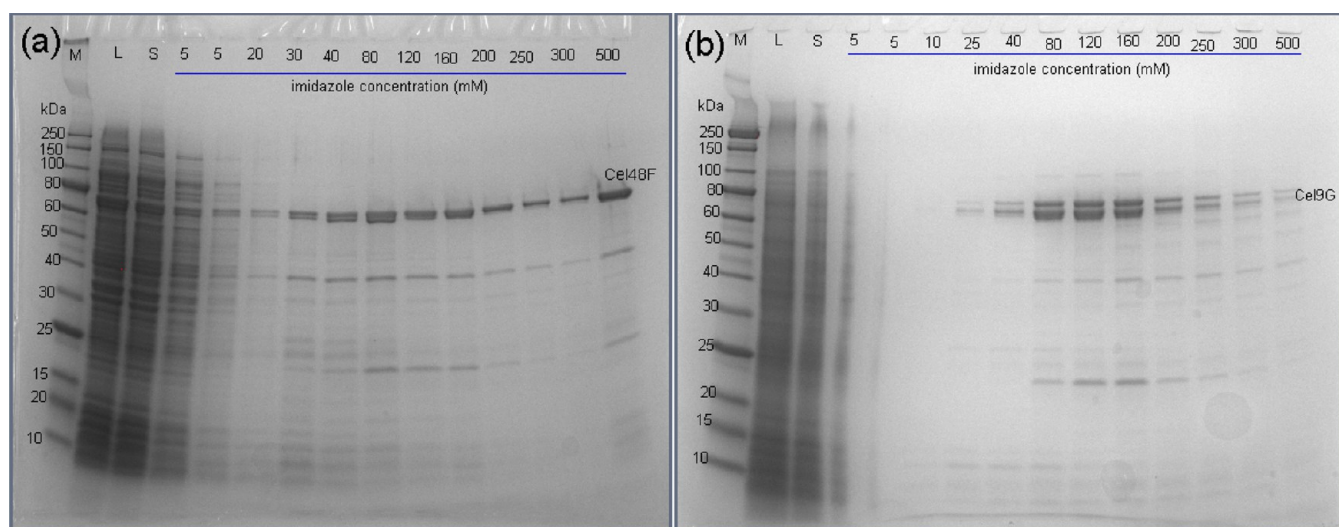


Figure 5. SDS-PAGE analysis of proteins separated from crude *E. coli* lysate containing His-tagged (a) Cel48F and (b) Cel9G treated with Ni-MNPs-3, respectively. Lane (M) is a molecular weight marker; Lane (L) is crude *E. coli* lysate; Lane (S) is the supernatant; the other lanes are proteins eluted from the Ni-MNPs-3 by buffers containing increasing amount of imidazole (from 5 to 500 mM).

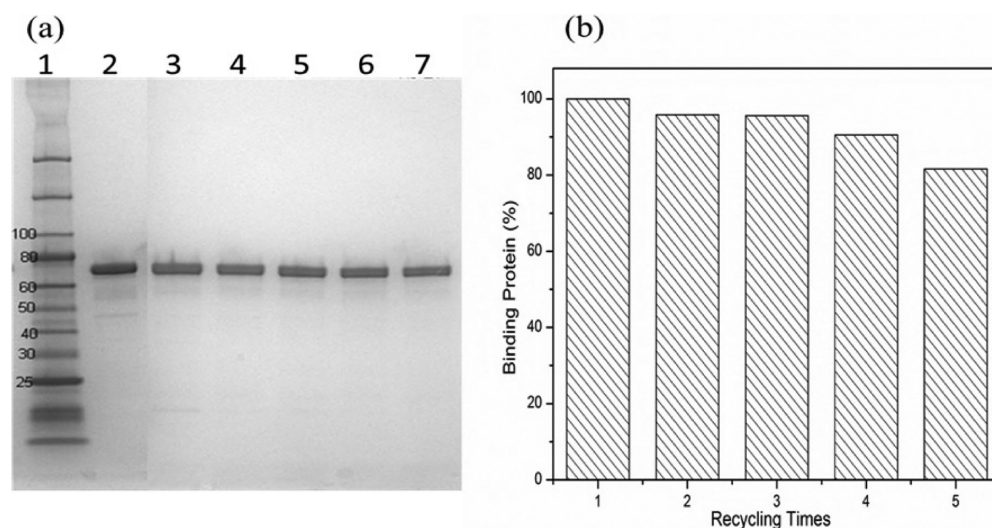


Figure 6. (a) SDS-PAGE analysis of proteins released from the Ni-MNPs-3 reused up to five times (Lanes 3–7). Lane 1 is a molecular weight marker; Lane 2 is the pure His-tagged Cel48F before separation. (b) Recycling of the Ni-MNPs-3 in the separation of His-tagged Cel48F.

which agrees with the result obtained from TGA analysis. The magnetic susceptibility of $\text{Fe}_3\text{O}_4/\text{PMG}$ is large enough to facilitate the quick separation of particles from solution (<30 s) using a regular magnetic plate (Supporting Information Figure S2).

3.3. Synthesis of $\text{Fe}_3\text{O}_4/\text{PMG}/\text{IDA}-\text{Ni}^{2+}$. The amino-epoxy ring-opening reaction was chosen to functionalize the composite microspheres. Here, we used IDA to open the epoxy ring in PMG. The “graft-on” process was characterized by monitoring of the zeta potential of microspheres in water. The $\text{Fe}_3\text{O}_4/\text{PMG}$ microspheres were weakly charged (−3 mV), and IDA modified $\text{Fe}_3\text{O}_4/\text{PMG}$ -IDA microspheres exhibited much larger negative zeta potential (−30 mV) as a result of the carboxyl groups of IDA grafted on the surface. To quantify the amount of IDA grafted on the surface, TGA analysis has been carried out and the result was shown in Figure 4a. The difference between curves (iii) and (iv) in Figure 4a was attributed to the grafted IDA, and the amount was calculated to be approximately 18 wt %. Ni^{2+} was then incorporated onto the

microspheres via the chelation of Ni^{2+} to the carboxylic groups and amino groups of IDA, leaving the remaining three metal-chelating sites for binding to the His-tagged proteins (the complexation mechanism is illustrated in Scheme 1). The amount of Ni^{2+} on the surface of $\text{Fe}_3\text{O}_4/\text{PMG}/\text{IDA}-\text{Ni}^{2+}$ (Ni-MNPs) was further quantified by atomic absorption spectroscopy (AAS) (Table 2). The $\text{Fe}_3\text{O}_4/\text{PMG}$ alone cannot be complex with Ni^{2+} ; only after reaction with IDA, Ni^{2+} can be immobilized on the microspheres. As expected, Ni-MNPs-3 contains more Ni^{2+} than the other two samples, and it is attributed to more abundant epoxy groups on the magnetic core. On the basis of the measured amount of bound Ni^{2+} , the epoxy groups (GMA amount) available on the surface of $\text{Fe}_3\text{O}_4/\text{PMG}$ -1, $\text{Fe}_3\text{O}_4/\text{PMG}$ -2 and $\text{Fe}_3\text{O}_4/\text{PMG}$ -3 were estimated to be 8.6, 16, and 16.8 wt %, respectively. Since it has high binding capacity of Ni^{2+} , Ni-MNPs-3 was used in the separation and purification of His-tagged cellulolytic enzymes in the following experiments.

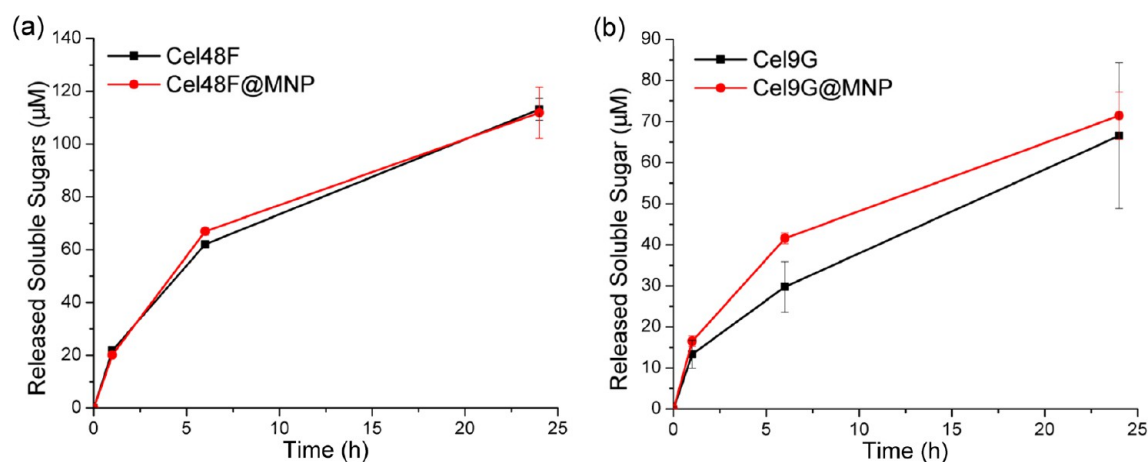


Figure 7. Avicel hydrolysis by cellulases (a) Cel48F and (b) Cel9G in the free state or immobilized on the magnetic microspheres (MNP). The amounts of reducing sugars were determined by the ferricyanide method, after incubation at 37 °C for 0, 1, 6, and 24 h. The final protein concentration was 0.02 μM in both free and immobilized states. The data show the mean of three independent experiments.

3.4. Application in Protein Separation. We first tested the binding of Ni-MNPs-3 with purified His-tagged Cel48F, which has a molecular weight of 80.7 kDa (722 amino acids). Almost all the His-tagged Cel48F can be isolated by Ni-MNPs-3 and be subsequently released from the microspheres by elution with imidazole as shown in the SDS-PAGE (Supporting Information Figure S3). We determined the binding capacity of Ni-MNPs-3 to be around 103 mg/g (protein/beads).

To demonstrate the practical applications of Ni-MNPs-3, we used them to isolate His-tagged enzymes directly from crude *E. coli* lysate. The separation process is illustrated in Scheme 2. Figure 5 demonstrates the purification performances of Ni-MNPs-3 for two His-tagged cellulases (Cel48F and Cel9G) expressed in *E. coli*. The His-tagged Cel48F protein was separated from the lysate with only a small amount of nonspecific bound proteins (Figure 5a). Imidazole (500 mM) was required to completely release those His-tagged Cel48F proteins bound on Ni-MNPs-3. Similarly, the His-tagged Cel9G protein (79.2 kDa) was separated from the cell lysate, although two protein bands were shown on SDS-PAGE due to protease cleavage during cell lysis. About 160 mM imidazole was needed to elute most His-tagged Cel9G proteins from Ni-MNPs-3 (Figure 5b). The results show that Ni-MNPs-3 has good binding specificity against other proteins in the *E. coli* lysates.

The recyclability of the magnetic microspheres in His-tagged protein separation was tested (Figure 6). After each separation, the magnetic microspheres were rinsed with buffer solution (50 mM Tris, pH 8.0, 300 mM NaCl, and 5 mM imidazole) for three times to wash out the excess imidazole and clean the surface of the particles. Recycling experiments were carried out for five times. The recyclability of Ni-MNPs-3 was evaluated by comparing the amount of collected Cel48F each time by normalizing the amount of Cel48F isolated in the first cycle. After five separation cycles, the separation capacity of the His-tagged protein was about 100%, 96%, 96%, 92%, and 81%, respectively (Figure 6b), which shows excellent recyclability for these kinds of composite microspheres in the separation of His-tagged proteins.

3.5. Enzyme Activity of Magnetic Microsphere-Immobilized Cellulases. The enzyme activity of the cellulases Cel48F and Cel9G on Avicel (20 mg/mL) was determined by evaluation of the total soluble reducing sugars

released at specific time intervals (incubation for 0, 1, 6, and 24 h), either in the free state or immobilized on the magnetic microspheres. After incubation for 24 h, $113 \pm 4 \mu\text{M}$ of reducing sugars were produced by Cel48F in the free state, whereas $112 \pm 10 \mu\text{M}$ of reducing sugars were released by Cel48F immobilized on the magnetic microspheres (Figure 7a). Similarly, $71 \pm 6 \mu\text{M}$ and $67 \pm 17 \mu\text{M}$ of reducing sugars were produced by Cel9G in its free and immobilized states after incubation for 24 h, respectively (Figure 7b). Clearly, the immobilized cellulases retain their enzymatic activity on the surface of the magnetic microspheres.

4. CONCLUSION

In summary, we have developed a cost-effective method for the synthesis of $\text{Fe}_3\text{O}_4/\text{PMG}$ core/shell microspheres by distillation–precipitation polymerization. The resulting $\text{Fe}_3\text{O}_4/\text{PMG}$ microspheres possess a well-defined core/shell structure, high magnetization, and high surface density of epoxy groups. Subsequently, IDA was used to open the epoxy rings to facilitate the complexation with Ni^{2+} at room temperature. The Ni^{2+} on the surface of microspheres provides abundant docking sites for histidine, and the composite microspheres exhibit excellent performance in the separation of His-tagged cellulases with a binding capacity as high as 103 mg/g. The presence of the superparamagnetic core in the microspheres allows them to be quickly isolated by an external magnetic field, facilitating the postprocessing and recycling. Ni-MNPs display high recyclability and stability for purification of His-tagged proteins over several separation cycles. A practical application of the microspheres was successfully demonstrated by separating His-tagged cellulases directly from *E. coli* lysate. The IDA– Ni^{2+} functionalized core/shell $\text{Fe}_3\text{O}_4/\text{PMG}$ magnetic nanocomposites may find potential applications in protein purification and direct immobilization of enzyme. Considering the simple synthesized processing and the low cost, the process is readily adaptable for industrial scales.

■ ASSOCIATED CONTENT

Supporting Information

Powder XRD patterns of MCNCs and $\text{Fe}_3\text{O}_4/\text{PMG}$. Magnetic separation behaviors of $\text{Fe}_3\text{O}_4/\text{PMG}$. SDS-PAGE analysis of proteins separated from pure His-tagged Cel48F. This material is available free of charge via the Internet at <http://pubs.acs.org>.

■ AUTHOR INFORMATION

Corresponding Author

*Telephone: +86-21-55664371 (C.W.). Fax: +86-21-65640293 (C.W.). E-mail: ccwang@fudan.edu.cn (C.W.); ylin@ims.uconn.edu (Y.L.).

Notes

The authors declare no competing financial interest.

■ ACKNOWLEDGMENTS

This work was supported by National Science and Technology Key Project of China (Grant No. 2012AA020204); National Science Foundation of China (Grant Nos. 21034003, 21128001, and 51073040). Y.L. acknowledges the UConn faculty start-up funds and a senior visiting scholarship provided by Fudan University.

■ REFERENCES

- (1) Dyal, A.; Loos, K.; Noto, M.; Chang, S.; Spagnoli, C.; Shafi, K. V. P. M.; Ulman, A.; Cowman, M.; Gross, R. A. *J. Am. Chem. Soc.* **2003**, *125*, 1684–1685.
- (2) Ma, W. F.; Zhang, Y.; Li, L. L.; You, L. J.; Zhang, P.; Zhang, Y. T.; Li, J. M.; Yu, M.; Guo, J.; Lu, H. J.; Wang, C. C. *ACS Nano* **2012**, *6*, 3179–3188.
- (3) Rembsum, A.; Dreyer, W. *Science* **1980**, *208*, 364–368.
- (4) Wang, D.; He, J.; Rosenzweig, N.; Rosenzweig, Z. *Nano Lett.* **2004**, *4*, 409–413.
- (5) Yang, J.; Lee, C. H.; Park, J.; Seo, S.; Lim, E. K.; Song, Y. J.; Suh, J. S.; Yoon, H. G.; Huh, Y. M.; Haam, S. *J. Mater. Chem.* **2010**, *20*, 8624–8630.
- (6) Kim, J.; Piao, Y.; Hyeon, T. *Chem. Soc. Rev.* **2009**, *38*, 372–390.
- (7) Shi, D. L.; Bedford, N. M.; Cho, H. S. *Small* **2011**, *7*, 2549–2567.
- (8) Luo, B.; Xu, S.; Luo, A.; Wang, W. R.; Wang, S. L.; Guo, J.; Lin, Y.; Zhao, D. Y.; Wang, C. C. *ACS Nano* **2011**, *5*, 1428–1435.
- (9) Cho, H. S.; Dong, Z. Y.; Pauletti, G. M.; Zhang, J. M.; Xu, H.; Gu, H. C.; Wang, L. M.; Ewing, R. C.; Huth, C.; Wang, F.; Shi, D. L. *ACS Nano* **2010**, *4*, 5398–5404.
- (10) Li, D.; Tang, J.; Wei, C.; Guo, J.; Wang, S. L.; Chaudhary, D.; Wang, C. C. *Small* **2012**, *8*, 2690–2697.
- (11) Ohlan, A.; Singh, K.; Chandra, A.; Dhawan, S. K. *ACS Appl. Mater. Interfaces* **2010**, *2*, 927–933.
- (12) Xu, S.; Ma, W. F.; You, L. J.; Li, J. M.; Guo, J.; Hu, J. J.; Wang, C. C. *Langmuir* **2012**, *28*, 3271–3278.
- (13) Liu, X. Q.; Guan, Y. P.; Ma, Z. Y.; Liu, H. Z. *Langmuir* **2004**, *20*, 10278–10282.
- (14) Butun, V.; Atay, A.; Tuncer, C.; Bas, Y. *Langmuir* **2011**, *27*, 12657–12665.
- (15) Nagao, D.; Yokoyama, M.; Yamauchi, N.; Matsumoto, H.; Kobayashi, Y.; Konno, M. *Langmuir* **2008**, *24*, 9804–9808.
- (16) Mu, L.; Liu, Y.; Cai, S. Y.; Kong, J. L. *Chem.—Eur. J.* **2007**, *13*, 5113–5120.
- (17) Liu, B.; Zhang, W.; Yang, F. K.; Feng, H. L.; Yang, X. L. *J. Phys. Chem. C* **2011**, *115*, 15875–15884.
- (18) Li, G. L.; Shi, Q.; Yuan, S. J.; Neoh, K. G.; Kang, E. T.; Yang, X. L. *Chem. Mater.* **2010**, *22*, 1309–1317.
- (19) Ma, W. F.; Zhang, Y.; Li, L. L.; Zhang, Y. T.; Yu, M.; Guo, J.; Lu, H. J.; Wang, C. C. *Adv. Funct. Mater.* **2013**, *23*, 107–115.
- (20) Ma, W. F.; Wu, K. Y.; Tang, J.; Li, D.; Wei, C.; Guo, J.; Wang, S. L.; Wang, C. C. *J. Mater. Chem.* **2012**, *22*, 15206–15214.
- (21) Bai, F.; Yang, X. L.; Li, R.; Huang, B.; Huang, H. Q. *Polymer* **2006**, *47*, 5775–5784.
- (22) Ji, M.; Liu, H. L.; Yang, X. L. *Polym. Chem.* **2011**, *2*, 148–156.
- (23) Zhang, H.; Yang, X. L. *Polym. Chem.* **2010**, *1*, 670–677.
- (24) Zhen, G.; Falconnet, D.; Kuennemann, E.; Voros, J.; Spencer, N. D.; Textor, M.; Zurcher, S. *Adv. Funct. Mater.* **2006**, *16*, 243–251.
- (25) Arnau, J.; Lauritzen, C.; Peterson, G. E.; Pedersen, J. *Protein Expression Purif.* **2006**, *48*, 1–13.
- (26) Nata, I. F.; El-Safory, N. S.; Lee, C. K. *ACS Appl. Mater. Interfaces* **2011**, *3*, 3342–3349.
- (27) Gaberc-Porekar, V.; Menart, V. *J. Biochem. Biophys. Methods* **2001**, *49*, 335–360.
- (28) Zhang, Z. J.; Wang, Z. L.; Chakoumakos, B. C.; Yin, J. S. *J. Am. Chem. Soc.* **1998**, *120*, 1800–1804.
- (29) Sun, S. H.; Murray, C. B.; Weller, D.; Folks, L.; Moser, A. *Science* **2000**, *287*, 1989–1992.
- (30) Perez, J. M.; Simeone, F. J.; Saeki, Y.; Josephson, L.; Weissleder, R. *J. Am. Chem. Soc.* **2003**, *125*, 10192–10193.
- (31) Xu, Y. L.; Qin, Y.; Palchoudhury, S.; Bao, Y. P. *Langmuir* **2011**, *27*, 8990–8997.
- (32) Xu, C.; Xu, K.; Gu, H.; Zhong, X.; Guo, Z.; Zheng, R.; Zhang, X.; Xu, B. *J. Am. Chem. Soc.* **2004**, *126*, 3392–3393.
- (33) Xu, C.; Xu, K.; Gu, H.; Zheng, R.; Liu, H.; Zhang, X.; Guo, Z.; Xu, B. *J. Am. Chem. Soc.* **2004**, *126*, 9938–9939.
- (34) Wang, W.; Wang, C.; Li, Z. *Chem. Commun.* **2011**, *47*, 8115–8117.
- (35) Kim, J.; Piao, Y.; Lee, N.; Park, Y. I.; Lee, I. H.; Lee, J. H.; Paik, S. R.; Hyeon, T. *Adv. Mater.* **2010**, *22*, 57–60.
- (36) Xu, F.; Geiger, J. H.; Baker, G. L.; Bruening, M. L. *Langmuir* **2011**, *27*, 3106–3112.
- (37) Li, Y. C.; Lin, Y. S.; Tsai, P. J.; Chen, C. T.; Chen, W. Y.; Chen, Y. C. *Anal. Chem.* **2007**, *79*, 7519–7525.
- (38) Herdt, A. R.; Kim, B. S.; Taton, T. A. *Bioconjugate Chem.* **2007**, *18*, 183–189.
- (39) Kim, J. S.; Valencia, C. A.; Liu, R. H.; Lin, W. B. *Bioconjugate Chem.* **2007**, *18*, 333–341.
- (40) Shukoor, M. I.; Natalio, F.; Therese, H. A.; Tahir, M. N.; Ksenofontov, V.; Panthofer, M.; Eberhardt, M.; Theato, P.; Schroder, H. C.; Müller, W. E. G.; Tremel, W. *Chem. Mater.* **2008**, *20*, 3567–3573.
- (41) Fang, W. J.; Chen, X. L.; Zheng, N. F. *J. Mater. Chem.* **2010**, *20*, 8624–8630.
- (42) Reverbel-Leroy, C.; Pages, S.; Belaich, A.; Belaich, J. P.; Tardif, C. *J. Bacteriol.* **1997**, *179*, 46–52.
- (43) Gal, L.; Gaudin, C.; Belaich, A.; Pages, S.; Tardif, C.; Belaich, J. P. *J. Bacteriol.* **1997**, *179*, 6595–6601.
- (44) Park, J. T.; Johnson, M. J. *J. Biol. Chem.* **1949**, *181*, 149–151.
- (45) Ge, J. P.; Hu, Y. X.; Biasini, M.; Beyermann, W. P.; Yin, Y. D. *Angew. Chem., Int. Ed.* **2007**, *46*, 4342–4345.
- (46) Fang, X. L.; Chen, C.; Jin, M. S.; Kuang, Q.; Xie, Z. X.; Xie, S. Y.; Huang, R. B.; Zheng, L. S. *J. Mater. Chem.* **2009**, *19*, 6154–6160.
- (47) Ma, W. F.; Xu, S.; Li, J. M.; Guo, J.; Lin, Y.; Wang, C. C. *J. Polym. Sci., Part A: Polym. Chem.* **2011**, *49*, 2725–2733.